

# Fragmentations and reactions of protonated *O,O*-dimethyl ethylphosphonate and some isotopomers produced by electrospray ionisation in an ion trap mass spectrometer

A.J. Bell<sup>a</sup>, F. Ferrante<sup>b</sup>, S.E. Hall<sup>c</sup>, V. Mikhailov<sup>c</sup>, D. Mitchell<sup>d</sup>,  
C.M. Timperley<sup>a</sup>, P. Watts<sup>a,\*</sup>, N. Williams<sup>a</sup>

<sup>a</sup> *Dstl Porton Down, Salisbury, Wilts SP4 0JQ, UK*

<sup>b</sup> *Dipartimento di Chimica Fisica "F. Accascina", Università, degli Studi di Palermo, 90128 Palermo, Italy*

<sup>c</sup> *School of Physics and Astronomy, University of Birmingham, Edgbaston, Birmingham B15 2TT, UK*

<sup>d</sup> *Department of Chemistry, Southampton University, Southampton SO7 1BJ, UK*

Received 22 June 2007; received in revised form 31 August 2007; accepted 6 September 2007

Available online 14 September 2007

## Abstract

The fragmentation behaviour of protonated *O,O*-dimethyl ethylphosphonate and its isotopomers deuterated in the  $\alpha$ - and  $\beta$ -positions of the ethyl group and their fragment ions, particularly  $\text{EtP}(\text{O})\text{OMe}^+(\text{IV})$ , have been investigated both experimentally in an ion trap mass spectrometer and theoretically by electronic structure calculations at the B3LYP level. Of particular interest is the finding that the phosphonium ion **IV** eliminates ethene with hydrogen/deuterium loss from both the  $\alpha$ - and  $\beta$ -positions. The initial step for both routes involves ethyl migration from P to O to form the ion  $\text{MeOP}^+\text{OEt}$  which then loses ethene by two mechanisms, both of which lead to the same products. That a unitary branching ratio for  $\alpha$ - and  $\beta$ -elimination is not observed indicates that although the final step of dissociation into product ion and ethene is energetically the most demanding, it is not rate limiting and the large entropy change associated with the dissociation allows earlier processes to determine the branching ratio. This demonstrates once again that free energy, not enthalpy (or energy), determines the course of gas phase ion processes.

© 2007 Elsevier B.V. All rights reserved.

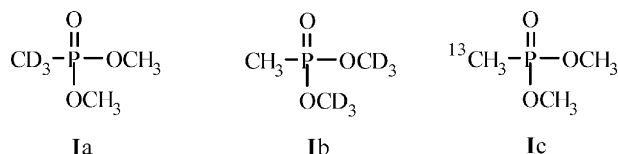
**Keywords:** Mass spectrometry; Electrospray; Ion trap; Organophosphates; Fragmentations

## 1. Introduction

In an initial investigation into the electrospray ionisation ion trap mass spectrometry of simple organophosphates esters [1], we reported that the collision induced fragmentation of protonated dimethyl methylphosphonate, **IH**<sup>+</sup>, resulted in the loss of methanol and the formation of the  $\text{CH}_3\text{P}(\text{O})\text{OCH}_3^+$  ion, **II**, which in turn fragmented under appropriate collision induced dissociation (CID) conditions to lose  $\text{CH}_2\text{O}$ .

It was observed that fragmentation of the deuterated ion  $\text{CD}_3\text{P}(\text{O})\text{OCH}_3^+$  formed from an isotopomer of **I**, **Ia** (see below) produces a mixture of  $\text{CH}_2\text{O}$  and  $\text{CD}_2\text{O}$ , indicating that a scrambling of the methyl groups is involved during fragmentation. More detailed studies of this scrambling involving the iso-

topomers **Ia**, **Ib** and **Ic**

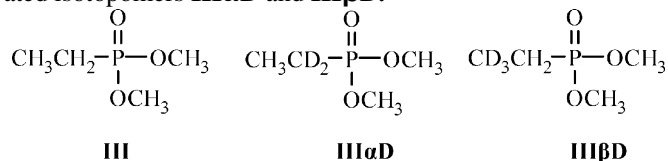


were made [2]. Subsequently, the scrambling of the methyl groups on elimination of formaldehyde from **II** was investigated using quantum mechanical calculations at the B3LYP and MP2 levels in an attempt to understand the mechanism(s) of fragmentation of **II** [3]. This was proposed in the paper describing the original experimental work [2] to occur through the dimethoxyphosphonium ion  $\text{P}(\text{OMe})_2^+$  formed from  $\text{MeP}(\text{O})\text{OMe}^+$  via a 1,2-methyl migration. 1,4-H migrations in both  $\text{MeP}(\text{O})\text{OMe}^+$  and  $\text{P}(\text{OMe})_2^+$  were proposed to explain the elimination of formaldehyde. The electronic structure calculations showed that the barriers to the origi-

\* Corresponding author. Tel.: +44 1980 862 161.

E-mail address: [pwatts.rsg@emailitis.com](mailto:pwatts.rsg@emailitis.com) (P. Watts).

nally proposed 1,4-H migration steps leading to loss of CH<sub>2</sub>O are much higher in energy than 1,3-H migrations in which a methoxy hydrogen atom migrates to the phosphorus atom. These produce the ion–dipole complexes CH<sub>2</sub>O·(MeP(O)H)<sup>+</sup> and CH<sub>2</sub>O·(MePOH)<sup>+</sup> which then dissociate to give the experimentally observed products. The present paper reports similar studies on *O,O*-dimethyl ethylphosphonate (**III**) and its deuterated isotopomers **IIIαD** and **IIIβD**.



## 2. Experimental

Compounds **III**, **IIIαD** and **IIIβD** were prepared by the Michaelis–Becker reaction [4] which involved deprotonating dimethyl phosphite with sodium hydride or *n*-butyllithium in tetrahydrofuran and alkylating the resultant anion with the respective iodoethane. Yields were very low, the result of carrying out the experiments on a small-scale, which complicated purification, and the tendency of dimethyl phosphite to *O*-dealkylate under such conditions [5]. Products were confirmed pure by <sup>1</sup>H and <sup>13</sup>C NMR spectroscopy and those containing deuterium labels by additional <sup>2</sup>H NMR spectroscopy.

Reagents were from Aldrich Ltd. (Gillingham, UK). Anhydrous solvents were employed: tetrahydrofuran was distilled from sodium/benzophenone. Thin layer chromatography (TLC) was used to monitor reactions using TLC plates (MK6F silica gel 60Å, 2.5 cm × 7.5 cm, layer thickness 250 μg) from Whatman (Maidstone, UK). Products were visualised by dipping the plates into a dilute solution of potassium permanganate in acetone: spots appeared white on a purple background. Silica gel for flash chromatography was from BDH Laboratory Supplies (Poole, UK). NMR spectra were obtained on a JEOL Lambda 500 instrument (operating at 500 MHz for <sup>1</sup>H, 77 MHz for <sup>2</sup>H, 126 MHz for <sup>13</sup>C, and 122 MHz for <sup>31</sup>P spectra) as solutions in CDCl<sub>3</sub> with internal reference SiMe<sub>4</sub> for <sup>1</sup>H and <sup>13</sup>C, and external trimethyl phosphite (δ 140 ppm) for <sup>31</sup>P spectra. Reactions were also monitored by gas chromatography–mass spectrometry (GC–MS) using a Finnigan MAT GCQ instrument with chemical ionisation using methane as reagent gas.

### 2.1. Dimethyl ethylphosphonate (**III**)

Sodium hydride (0.44 g, 60% dispersion in oil, 18.3 mmol) was washed twice with hexane (2 × 5 ml) and dried under vacuum. It was suspended in THF (50 ml), cooled to 0 °C and a solution of dimethyl phosphite (2.0 g, 18.2 mmol) in THF (10 ml) added dropwise via a cannula with stirring. After 45 min, a solution of iodoethane (2.84 g, 18.2 mmol) in THF (10 ml) was added dropwise. The mixture was stirred at 0 °C for 15 min then at room temperature for 2 h. Water (5 ml) was added to dissolve the precipitated sodium iodide and the product extracted with ether (2 × 50 ml). The ether extracts were combined and dried (MgSO<sub>4</sub>). Analysis of an aliquot by GC–MS revealed the

presence of 85% product. The drying agent was filtered off and the filtrate concentrated. Bulb-to-bulb distillation of the residue gave the title compound as a colourless liquid (0.25 g, 10%). Bp 80 °C/10 mmHg. <sup>1</sup>H NMR: δ = 3.75 (6H, d, <sup>3</sup>J<sub>PH</sub> = 11 Hz, OCH<sub>3</sub>), 1.77 (4H, dq, <sup>2</sup>J<sub>PH</sub> = 19 Hz, <sup>3</sup>J<sub>HH</sub> = 8 Hz, P-CH<sub>2</sub>), 1.17 (6H, dt, <sup>3</sup>J<sub>PH</sub> = 20 Hz, <sup>3</sup>J<sub>HH</sub> = 8 Hz, CH<sub>3</sub>). <sup>13</sup>C NMR: δ = 52.3 (d, <sup>2</sup>J<sub>PC</sub> = 7 Hz, OCH<sub>3</sub>), 17.7 (d, <sup>1</sup>J<sub>PC</sub> = 143 Hz, P-CH<sub>2</sub>), 6.4 (d, <sup>2</sup>J<sub>PC</sub> = 7 Hz, CH<sub>3</sub>). <sup>31</sup>P NMR: δ = 36.9.

### 2.2. Dimethyl 1,1-*d*<sub>2</sub>-ethylphosphonate (**IIIαD**)

*n*-Butyllithium (5.7 ml of 1.6 M solution in hexanes, 9.06 mmol) was added dropwise by syringe to a stirred solution of dimethyl phosphite (1.0 g, 9.09 mmol) in THF (10 ml) at –78 °C. After 90 min, iodoethane-1,1-*d*<sub>2</sub> (1.44 g, 9.11 mmol) in THF (5 ml) was added via a cannula. The mixture was stirred at –78 °C for a further 30 min and then at room temperature for 2 h. Water (5 ml) was added to dissolve the precipitated sodium iodide and the product extracted with dichloromethane (3 × 10 ml). The organic extracts were combined and dried (MgSO<sub>4</sub>). The drying agent was filtered off and the filtrate concentrated. Column chromatography of the residue, eluting with 3:2 hexane–acetone, gave the title compound as a colourless liquid (100 mg, 8%). <sup>1</sup>H NMR: δ = 3.78 (6H, d, <sup>3</sup>J<sub>PH</sub> = 11 Hz, OCH<sub>3</sub>), 1.15 (3H, d, <sup>3</sup>J<sub>PH</sub> = 20 Hz, CD<sub>2</sub>CH<sub>3</sub>). <sup>2</sup>H NMR: δ = 2.11 (2D, s, CD<sub>2</sub>). <sup>13</sup>C NMR: δ = 52.2 (d, <sup>2</sup>J<sub>PC</sub> = 6 Hz, CD<sub>2</sub>CH<sub>3</sub>), 6.2 (d, <sup>2</sup>J<sub>PC</sub> = 6 Hz, CH<sub>3</sub>). <sup>31</sup>P NMR: δ = 36.9.

### 2.3. Dimethyl 2,2,2-*d*<sub>3</sub>-ethylphosphonate (**IIIβD**)

Prepared by the same method used for dimethyl ethylphosphonate but using iodoethane-2,2,2-*d*<sub>3</sub> instead of iodoethane. The title compound was obtained as a colourless liquid after bulb-to-bulb distillation under reduced pressure (206 mg, 8%). Bp 90 °C/12 mmHg. <sup>1</sup>H NMR: δ = 3.72 (6H, d, <sup>3</sup>J<sub>PH</sub> = 11 Hz, OCH<sub>3</sub>), 1.71 (2H, br d, <sup>2</sup>J<sub>PH</sub> = 18 Hz, P-CH<sub>2</sub>). <sup>2</sup>H NMR: δ = 1.17 (2D, dt, <sup>3</sup>J<sub>PD</sub> = 3 Hz, <sup>3</sup>J<sub>HD</sub> = 1 Hz, CD<sub>3</sub>). <sup>13</sup>C NMR: δ = 52.3 (d, <sup>2</sup>J<sub>PC</sub> = 6 Hz, OCH<sub>2</sub>), 17.5 (d, <sup>1</sup>J<sub>PC</sub> = 143 Hz, P-CH<sub>2</sub>). <sup>31</sup>P NMR: δ = 36.9.

The mass spectrometric technique has been described in detail elsewhere [2]. In this work only the Esquire~LC, Bruker Daltonics, GmbH ion trap mass spectrometer was used.

#### 2.3.1. Computational details

Geometry optimizations and frequency calculations of all species reported in this work were performed by using Density Functional Theory with the Becke three parameters hybrid functional B3LYP [6] and the triple-ζ basis set 6-311 + G(2d,2p), including polarisation and diffusion functions. In the DFT calculations, a grid of 99 radial point and 590 angular points, together with the Becke weighting scheme of integration, have been used. Vibrational frequencies were calculated in all cases to characterize the minima and the transition states and provide zero point energies (ZPE). All total energy comparison include ZPE corrections. Earlier studies on ions obtained from protonated dimethyl methylphosphonate [3] demonstrated that the results at the B3LYP level corresponded very well with those from the

more time-consuming MP2 calculations and that all ions have a singlet electronic ground state. All electronic structure calculations were performed using the Gaussian 03 programme [7].

### 3. Results

#### 3.1. Fragmentation of $\text{IIIH}^+$ and its product ions

These are summarised in Fig. 1. Only the ions with  $m/z$ s 139, 125, and 111 could be isolated and fragmented directly and the relevant spectra are shown in Figs. 2–4. The ions with  $m/z$ s 107, **IV** and 93, **V** reacted rapidly with the traces of water always present in the helium bath gas so that attempts to isolate them resulted in mixtures of ions with  $m/z$ s 107 and 125 and  $m/z$ s 93 and 111, respectively. They are, however, present in sufficient intensity after fragmentation of  $\text{IIIH}^+$  and  $m/z$  125 that they can be excited directly and the spectra are shown in Figs. 5 and 6.

Isolation and fragmentation of  $m/z$  140,  $\text{IIID}^+$  (produced when using  $\text{D}_2\text{O}$  in the spraying medium), gave ions with  $m/z$ s 125, 107 and 79. Isolation and fragmentation of  $m/z$  125 gave ions with  $m/z$ s 107, 93, and 79 with a trace of 111. Isolation and fragmentation of  $m/z$  111 gave ions with  $m/z$ s 93 and 65. Of importance was the observation that, in contrast to the fragmentation of **II**, no loss of formaldehyde from **IV** occurred.

Fragmentation of the deuterated isotopomers  $\text{III}\alpha\text{DH}^+$  and  $\text{III}\beta\text{DH}^+$  gave unexpected results. The deuterated isotopomers of **IV** and **V** produced ethene with the hydrogen/deuterium loss occurring from both the  $\alpha$ - and  $\beta$ -positions of the ethyl group. Thus fragmentation of  $\text{IV}\alpha\text{D}$ ,  $m/z$  109, gave ions with  $m/z$  79 and  $m/z$  80 corresponding to loss of  $\text{CD}_2\text{CH}_2$  ( $\beta$  loss) and  $\text{CHDCH}_2$

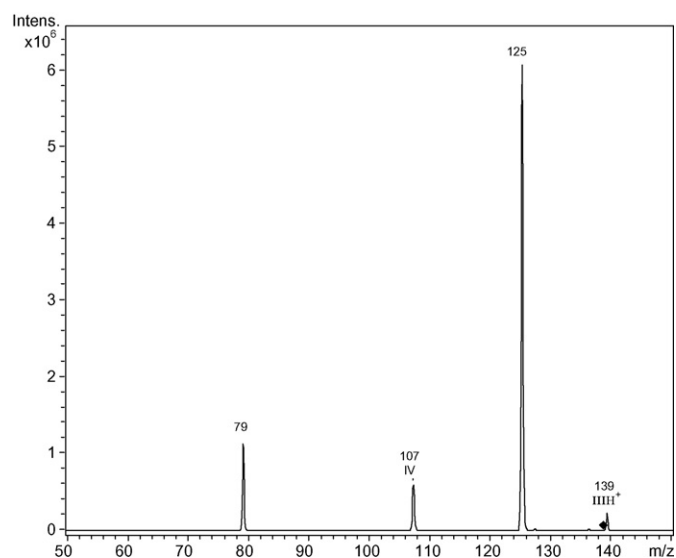


Fig. 2. Isolation and fragmentation of  $\text{IIIH}^+$ ,  $m/z$  139 (see Fig. 1).

( $\alpha$  loss), respectively. This is shown in Fig. 7. Fragmentation of  $\text{IV}\beta\text{D}$ ,  $m/z$  110, also gave ions with  $m/z$  79 and  $m/z$  80, this time corresponding to loss of  $\text{CD}_2\text{CHD}$  ( $\alpha$  loss) and  $\text{CD}_2\text{CH}_2$  ( $\beta$  loss), respectively and is shown in Fig. 8. Similar results were obtained for the fragmentations of  $\text{V}\alpha\text{D}$  and  $\text{V}\beta\text{D}$ . The difference in the  $\alpha/\beta$  loss ratios for the two isotopomers was initially ascribed to an isotope effect. Further studies indicated that whilst an isotope effect may be a contributing factor, it was not the dominant reason for the differing  $\alpha/\beta$  loss ratios. It was observed that the  $\alpha/\beta$  loss ratio was dependent upon the fragmentation time with the  $\alpha/\beta$  loss ratio decreasing with an increase in fragmentation time for the  $\alpha\text{D}$  isotopomer but increasing for the  $\beta\text{D}$  isotopomer. Moreover, if after fragmentation a scan delay (typically 20 ms) was inserted before a mass scan, the  $m/z$  80 peak disappeared with a concomitant increase of the  $m/z$  79 peak for both isotopomers. This is interpreted as the ions resulting from the loss of ethene whether from **IV** or **V** having a labile hydro-

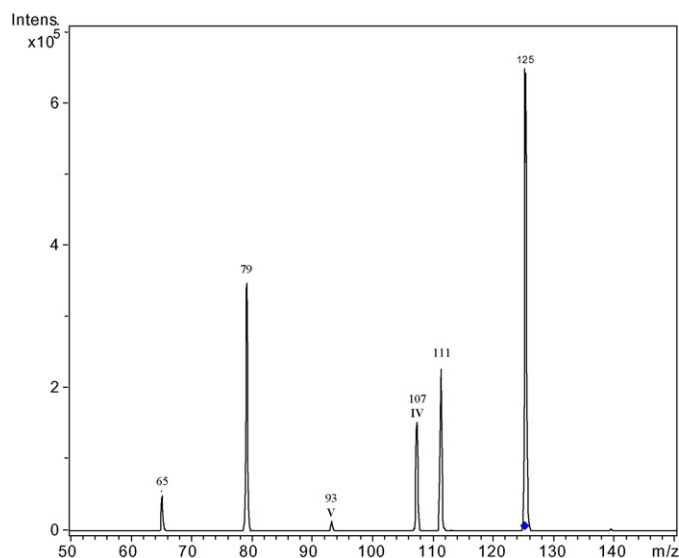


Fig. 3. Isolation and fragmentation of  $m/z$  125 (see Fig. 1).

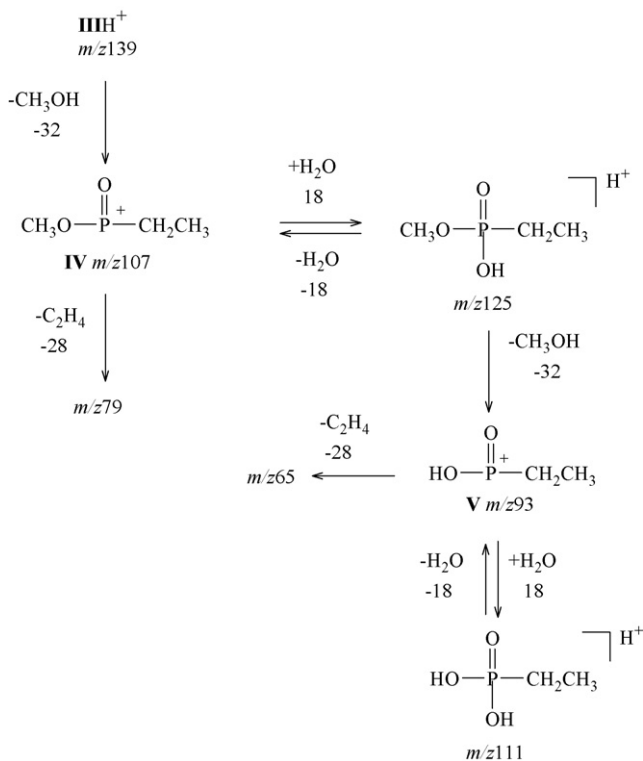
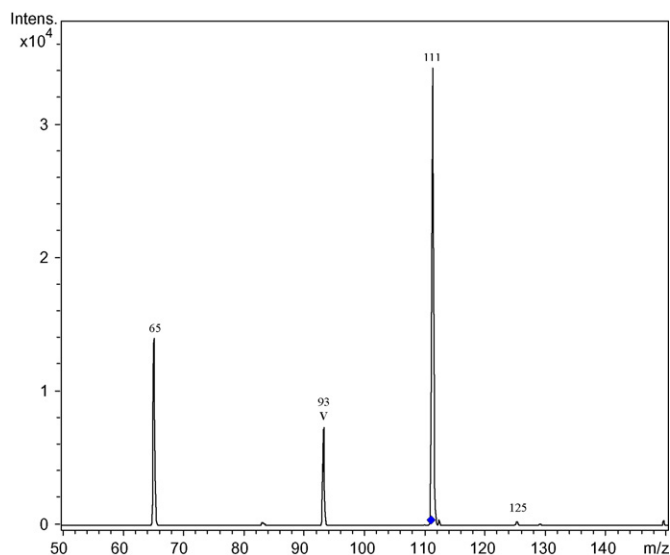
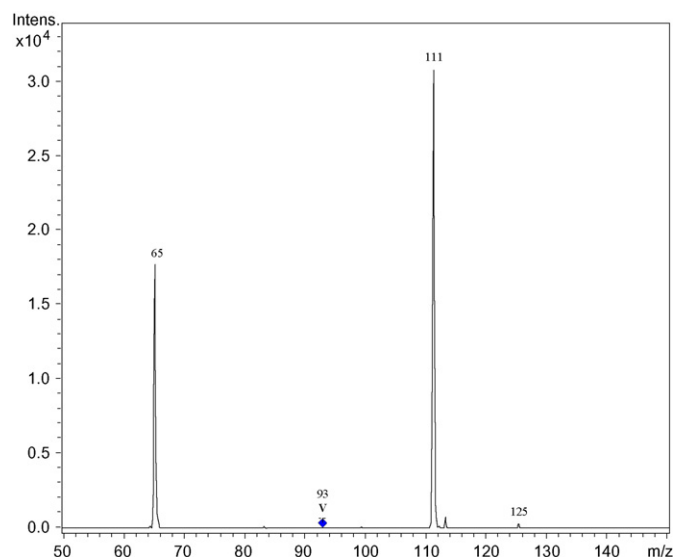
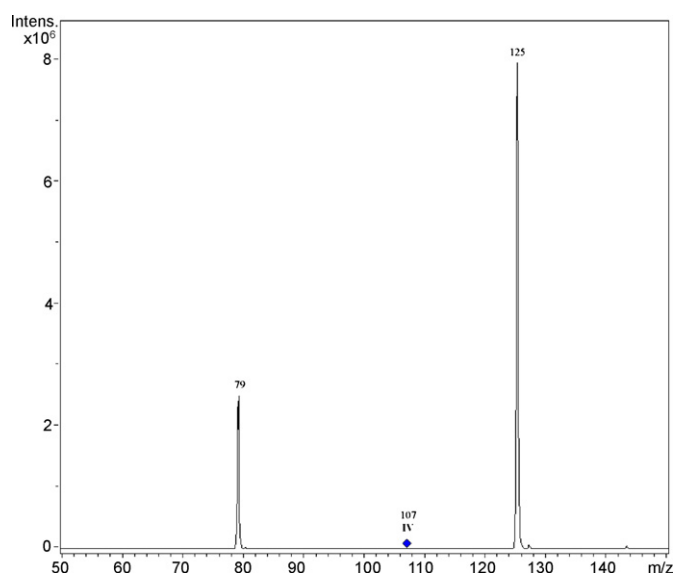
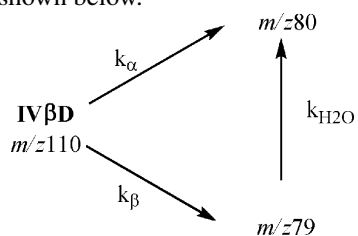
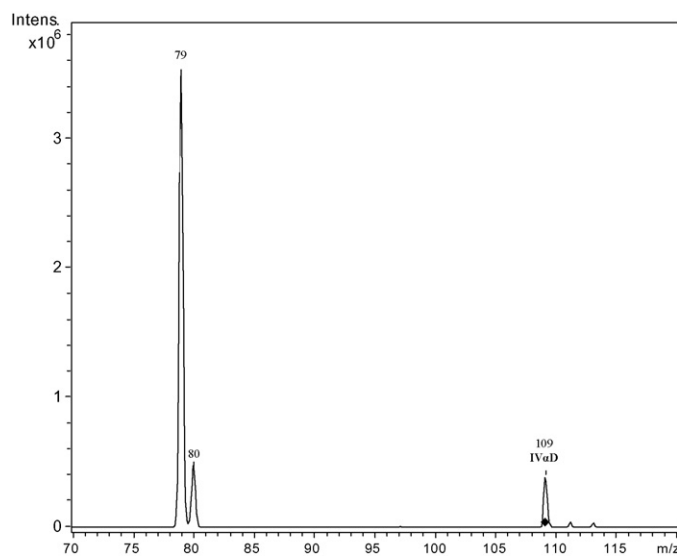


Fig. 1. Fragmentation of  $\text{IIIH}^+$  and its fragment ions.

Fig. 4. Isolation and fragmentation of  $m/z$  111 (see Fig. 1).Fig. 6. Isolation and fragmentation of V,  $m/z$  93 (see Fig. 1).

gen/deuterium. After formation, the ions with the higher  $m/z$  containing a deuterium i.e.,  $m/z$  80 and  $m/z$  66, lose the deuterium in exchange with the water present in the bath gas. This hydrogen/deuterium exchange is sufficiently rapid to occur during the fragmentation period thus accounting for the difference in the observed  $\alpha/\beta$  ratios for the two isotopomers. A schematic of the fragmentation reactions and D/H exchange for the  $\beta\text{D}$  isotopomer is shown below.

Fig. 5. Isolation and fragmentation of IV,  $m/z$  107 (see Fig. 1).Fig. 7. Fragmentation of IV $\alpha$ D,  $m/z$  109.

Modeling of this scheme using VisSim (Visual Solutions Inc., Westford, MA 01886, USA) and comparing the concentration time profiles with fragmentation spectra such as given in Figs. 7 and 8 suggests that, ignoring kinetic isotope effects,  $\alpha$ -elimination is about  $5\times$  slower than  $\beta$ -elimination and that, assuming hydrogen/deuterium exchange occurs at the collisional rate, the water concentration in the trap is ca. 10 ppm.

In the previous study, the ion of interest, **II**, could be isolated before fragmentation. It was proposed that on its excitation in the ion trap, not only were all of the ions **II** maintained at a suprathreshold temperature i.e., given an excess of internal energy, but also all of the ions formed by rearrangement of **II** (having the same  $m/z$ ) had the same excess of internal energy even if their formation from **II** was endothermic. This assumed that the rearranged ions had lifetimes consistent with their being intermediates and therefore subject to excitation; if they had much shorter lifetimes more consistent with their being transient

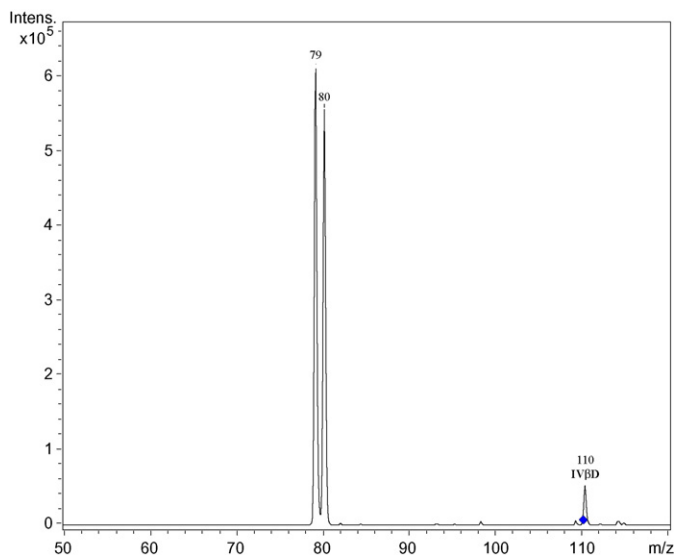


Fig. 8. Fragmentation of **IVBD**,  $m/z$  110.

species then the argument that they can increase their internal energy to that of **II** is nugatory.

As was noted above, because of their rapid reaction with water in the bath gas, the ions **IV** and **V** could not be isolated, although after fragmentation of **IIIH**<sup>+</sup> and  $m/z$  125 they can be excited directly. When the isotopomers are studied, the  $\alpha/\beta$  ratios i.e.,  $m/z$  79 and  $m/z$  80, are effectively independent of which ion is excited e.g., **III $\alpha$ DH**<sup>+</sup>, **IV $\alpha$ D**, and  $m/z$  127 although **III $\alpha$ DH**<sup>+</sup> and  $m/z$  127 require greater excite voltages than does **IV $\alpha$ D**. This finding demonstrates that the rearranged ions, at least in this instance, have only a transitory existence and do not acquire any additional energy before fragmentation.

### 3.2. Calculations

#### 3.2.1. General considerations – enthalpy or energy versus free energy

Although energies of species rather than enthalpies have been calculated for the present paper, no significant errors will be incurred in treating them as enthalpies in the discussions of mechanisms and courses of the reactions. The consideration of free energies rather than enthalpies is somewhat more difficult in the present system because of the difficulty in defining a temperature of the reacting species. Unless the ions are being excited it is probably safe to consider them to be approximately at the ambient temperature of the ion trap. But on excitation they can be at temperatures in excess of 1000 K [3]. Calculations show that for any particular precursor ion the entropies of its rearranged isomers and associated transition states are sufficiently similar to each other that the reaction coordinate has a similar profile irrespective of whether energy (or enthalpy) or free energy is used. But this is not the case when we come to the dissociation of the final complex to produce the fragmentation products. The entropy change is sufficiently large that although the dissociations are markedly endoergic, at the temperatures likely to be achieved on excitation they become exergonic. This will be seen to be of particular importance when

considering branching ratios, for both  $\alpha$ - and  $\beta$ -eliminations lead to the same products which have higher energies than the precursor ions and transition states associated with the various rearrangements/isomerisations. Thus, if energies/enthalpies were the parameter defining the reaction coordinate, the branching ratio should be unity. If however the final dissociation step is exergonic then the rate determining barriers occur on an earlier portion of the reaction coordinate where the energetics of  $\alpha$ - and  $\beta$ -eliminations for example are different thus leading to non-unitary branching ratios. Similar arguments can be applied to the elimination of water or methanol from  $m/z$  125—see later.

#### 3.2.2. Fragmentation of **IIIH**<sup>+</sup>

The proton affinities for the phosphoryl oxygen and the methoxy oxygen are 890 and 790 kJ mol<sup>-1</sup>, respectively, with the TS energy from the former to the latter being 180 kJ mol<sup>-1</sup>.

As was found in our previous studies [3,8] elimination of methanol from a protonated pentavalent phosphorus ester does not proceed *via* a transition state; bond breaking leads to two “non-interacting” molecules i.e., as the bond breaks the total energy does not show a maximum but increases to an asymptotic value. This energy is 125 kJ mol<sup>-1</sup> for elimination of methanol from **IIIH**<sup>+</sup> with the proton on the methoxy oxygen or 225 kJ mol<sup>-1</sup> from **IIIH**<sup>+</sup> with the proton on the phosphoryl oxygen. Although endoergic, this loss of methanol is quite facile due to the large entropy change, 171 J mol<sup>-1</sup> K<sup>-1</sup>. Despite its not being the primary product ion,  $m/z$  125 is the dominant product ion and is formed by rapid addition of water to **IV**.

#### 3.2.3. Fragmentation of $m/z$ 125 (see Fig. 1)

The ion  $m/z$  125 is a precursor of both **IV** and **V** making its fragmentation of interest.

The proton affinities for the phosphoryl oxygen, the hydroxyl oxygen and the methoxy oxygen are 890, 769 and 780 kJ mol<sup>-1</sup>, respectively; the transition state energies (TS) for their interconversions are given in Fig. 9. The energies for elimination of water and methanol are 91 and 144 kJ mol<sup>-1</sup>, respectively, from  $m/z$

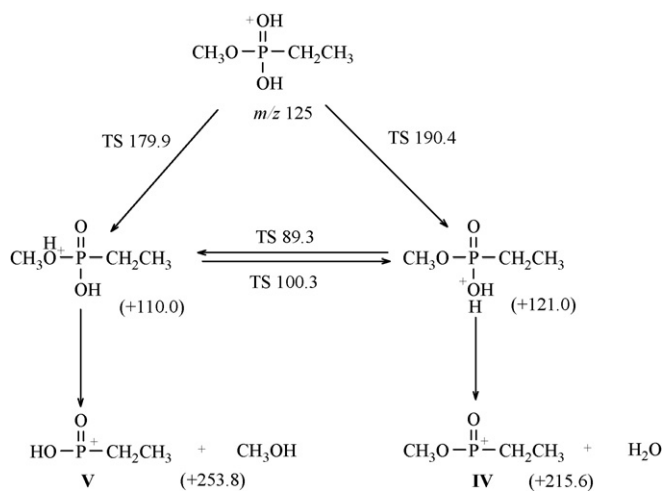


Fig. 9. Energies of species are referenced to  $m/z$  125 with the proton on the phosphoryl oxygen. TS energies are referenced to the starting species. All energies are in kJ mol<sup>-1</sup>.

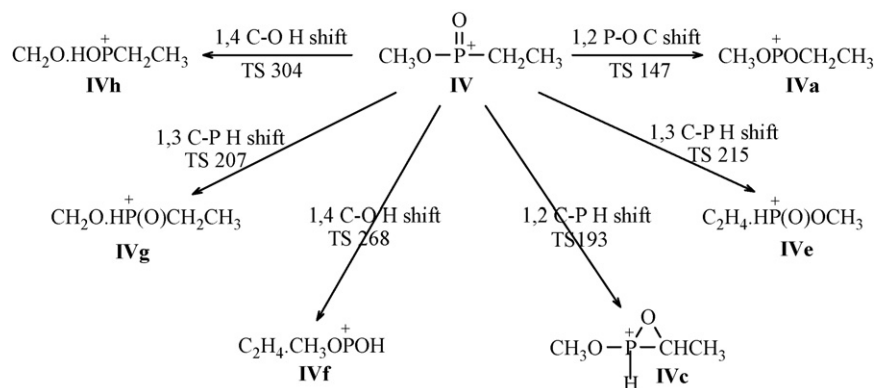


Fig. 10. Possible reactions of **IV** with associated TS energies in  $\text{kJ mol}^{-1}$ .

125 with the proton on the appropriate oxygen with the corresponding entropy changes being 122 and  $98 \text{ J mol}^{-1} \text{ K}^{-1}$ . The proton migrations and elimination of water or methanol are summarized in Fig. 9. It should be noted that although the ion with the proton on the phosphoryl oxygen has the lowest energy, it is unlikely to be the isomer present in the ion trap. This is because  $m/z$  125 is not formed in the electrospray source (unlike **IIIH**<sup>+</sup>) but is formed by reaction of **IV** with water and, when formed, is unlikely to have sufficient energy to overcome the transition states for proton migration. This uncertainty as to the position of the proton makes interpretation of the branching ratio for water versus methanol elimination difficult and this difficulty is further compounded by both **IV** and **V** reacting with water which in the case of **IV** reforms the starting ion.

As for the fragmentation of **IIIH**<sup>+</sup>, there is a large entropic contribution to the loss of both water and methanol. It is of interest that neither **IV** nor **V** can be formed without their fragmenting further with loss of ethene to  $m/z$ s 79 and 65, respectively.

#### 3.2.4. Fragmentation of **IV**

Electronic structure calculations suggest six energetically feasible intramolecular rearrangements/reactions of **IV**. These are shown in Fig. 10.

As before [3] there are two possible mechanisms for formaldehyde production, a 1,3 C-P H migration (**IV** → **IVg**) and a 1,4 C-O H migration (**IV** → **IVh**). The former has a TS energy of  $207 \text{ kJ mol}^{-1}$  and the latter a TS energy of

$304 \text{ kJ mol}^{-1}$  which are remarkably similar to the TS energies for the corresponding mechanisms for the fragmentation of **II** ( $211$  and  $312 \text{ kJ mol}^{-1}$ , respectively). As no formaldehyde is produced in the fragmentation of **IV** it is concluded that only the rearrangements/fragmentations of **IV** which have TS energies somewhat below  $200 \text{ kJ mol}^{-1}$  will be observed. This leaves only the ethyl migration from P to O **IV** → **IVa** and the cyclisation **IV** → **IVc**. The TS energy for the cyclisation is much higher than that for **IV** → **IVa** and is unlikely to compete. The reactions of **IVa** are shown in Fig. 11. It should be noted that the **IVc** and **IVe** appearing in Fig. 11 are formed via different routes to those given in Fig. 10. As suggested earlier the large entropy change associated with the dissociation of **IVe** is important i.e.,  $\Delta G$  rather than  $\Delta H$  is the driving force making the dissociation step non rate limiting thus allowing the non-unitary branching ratio for  $\alpha$ - and  $\beta$ -elimination. The calculated energies and entropies given in Table 2 suggest that kinetic isotope effects are negligible for both elimination pathways for the  $\alpha$ -deuterated isotopomer, but that a small reduction in  $\beta$ -elimination for the  $\beta$ -deuterated isotopomer may occur. But overall it is considered that potential kinetic isotope effects do not affect the conclusions from kinetic simulation the  $\beta$ -elimination is that preferred route.

The energies of species and transition states for the processes shown in Fig. 11 are given in Table 1.

These are shown in graphical form in Fig. 12.

Once the dissociation steps of the complex are discounted for the previously mentioned entropic considerations, it is clear that

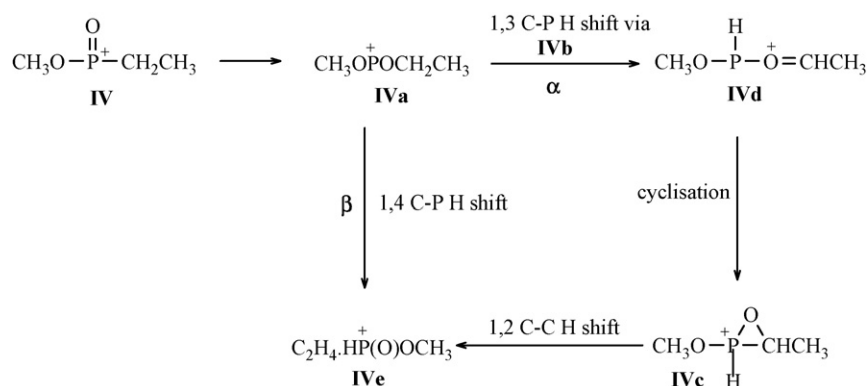


Fig. 11. Reactions of **IVa**. The  $\alpha$  and  $\beta$  refer from which position the hydrogen loss occurs (**IVb** is a conformational isomer of **IVa**).

Table 1  
Energies and entropies of species and transition states for the reactions shown in Fig. 11

| Species or TS        | Energy kJ mol <sup>-1</sup> | Entropy J K <sup>-1</sup> mol <sup>-1</sup> |
|----------------------|-----------------------------|---------------------------------------------|
| <b>IV</b>            | 0                           | 389.2                                       |
| <b>IVa</b>           | -8.6, -9.6, -8.3            | 382.5                                       |
| <b>IVb</b>           | -12.2, -13.2, -12.0         | 383.7                                       |
| <b>IVc</b>           | 111.3, 112.5, 111.5         | 367.0                                       |
| <b>IVd</b>           | 42.9, 44.5, 43.8            | 388.3                                       |
| <b>IVe (complex)</b> | 108.9                       | 429.7                                       |
| <b>Products</b>      | 190.6                       | 538.4                                       |
| TS IV → IVa          | 146.8, 147.3, 148.5         | 452.7                                       |
| TS IVa → IVe         | 146.2, 146.7, 151.4         | 411.7                                       |
| TS IVb → IVd         | 135.7, 138.3, 136.4         | 365.3                                       |
| TS IVc → IVe         | 176.3, 176.8, 178.7         | 370.3                                       |
| TS IVd → IVc         | 157.4, 159.1, 158.3         | 368.3                                       |

The first entry in the energy column is referenced to **IV**, the second to **IVαD**, and the third to **IVβD**.

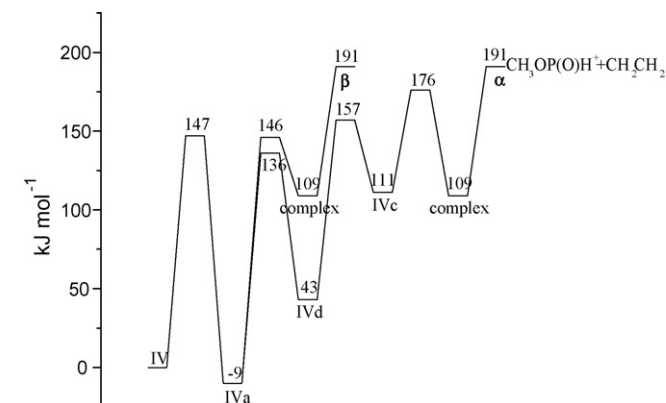


Fig. 12. Energetics for the fragmentation of **IV**.

$\alpha$ -elimination is going to be less favoured than  $\beta$ -elimination in accord with observation.

### 3.2.5. Fragmentation of **V**

The same set of arguments given for fragmentation of **IV** apply.

Electronic structure calculations suggest four energetically feasible intramolecular rearrangements of **V**. These together with their associated TS energies in kJ mol<sup>-1</sup> are shown in Fig. 13.

Table 2  
Energies and entropies of species and transition states for the reactions shown in Fig. 14

| Species or TS            | Energy kJ mol <sup>-1</sup> | Entropy J K <sup>-1</sup> mol <sup>-1</sup> |
|--------------------------|-----------------------------|---------------------------------------------|
| <b>V</b>                 | 0                           | 315.6                                       |
| <b>Va</b>                | -18.2, -14.4, -13.0         | 336.5                                       |
| <b>Vb</b>                | -16.2, -17.4, -16.0         | 338.2                                       |
| <b>Vc</b>                | 99.8, 100.9, 100.1          | 316.0                                       |
| <b>Vd</b>                | 26.9, 28.3, 27.8            | 345.7                                       |
| <b>Ve complex</b>        | 98.8                        | 343.1                                       |
| <b>Products</b>          | 204.4                       | 494.1                                       |
| TS <b>V</b> → <b>Va</b>  | 127.9, 128.4, 129.8         | 366.6                                       |
| TS <b>Va</b> → <b>Ve</b> | 141.2, 141.7, 146.4         | 340.2                                       |
| TS <b>Vb</b> → <b>Vd</b> | 117.1, 119.5, 117.8         | 324.4                                       |
| TS <b>Vc</b> → <b>Ve</b> | 142.5, 144.0, 143.4         | 326.9                                       |
| TS <b>Vd</b> → <b>Vc</b> | 155.1, 156.3, 158.0         | 318.9                                       |

The first entry in the boxes in the energy column is referenced to **V**, the second to **VαD**, and the third to **VβD**.

As for the fragmentation of **IV** the energetically most favourable pathway is the 1,2 P-O C shift to **Va** the reactions of which are shown in Fig. 14.

The energies of species and transition states for the processes shown in Fig. 14 are given in Table 2 and shown schematically in Fig. 15.

### 3.2.6. Structures and properties of the ions with $m/z$ 79/80 and $m/z$ 65/66

As was seen in Sections 3.2.4 and 3.2.5 discussing the fragmentations of **IV** and **V**, respectively, the hydrogen/deuterium originating from the ethyl group migrates to the phosphorus atom during the elimination of ethene. This is shown in Fig. 16 for the deuterium isotopomers.

Whilst however it is the deuterium atom that exchanges with hydrogen in water (any exchange with the hydrogen on the hydroxyl group in  $m/z$  66 will not be observed), the resulting ions  $m/z$  79 and  $m/z$  65 do not necessarily have the same structures as shown in Fig. 16 as the isomeric ions shown in Fig. 17 are more stable by 117 and 125 kJ mol<sup>-1</sup>, respectively.

It is suggested that it is these ions that result from the deuterium/hydrogen exchange/rearrangement of the ions with  $m/z$  80 and  $m/z$  66 (and of course with the H/H exchange that must occur with the non-deuterated isotopomeric ions). It is of interest that, as shown earlier, these structures cannot be accessed

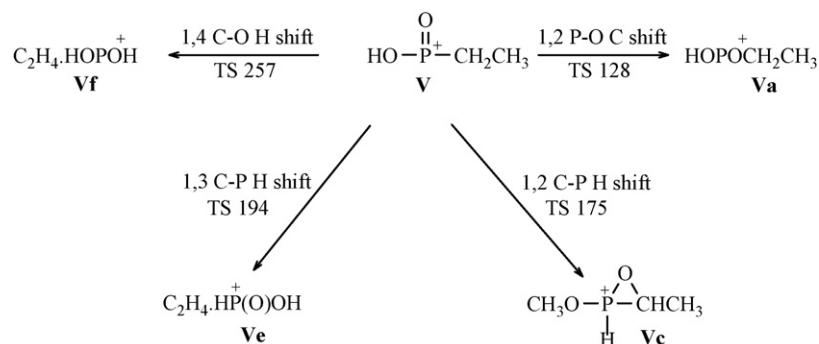


Fig. 13. Possible reactions of **V** and their associated TS energies in kJ mol<sup>-1</sup>.

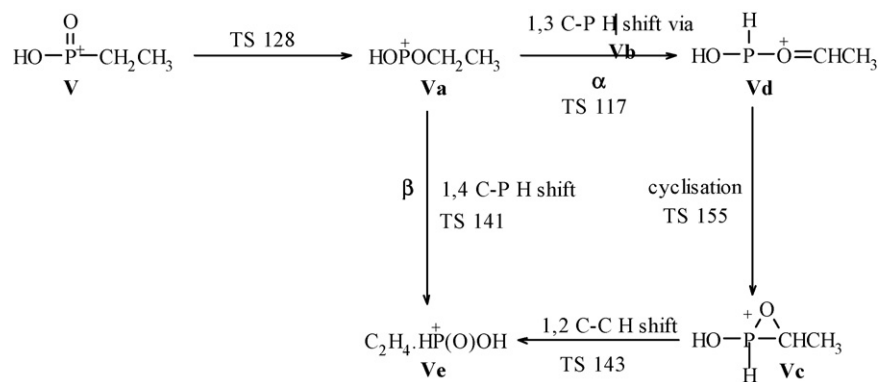


Fig. 14. Reactions of **Va**. The  $\alpha$  and  $\beta$  refer from which position the hydrogen loss occurs (**Vb** is a conformational isomer of **Va**).

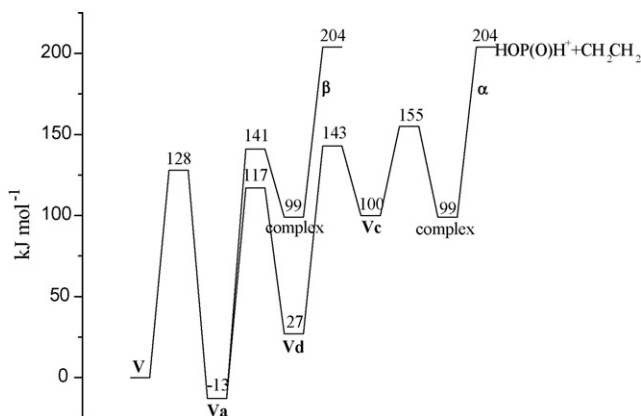


Fig. 15. Energetics for the fragmentation of **V**.

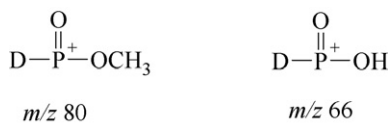


Fig. 16. Structures of the ions with  $m/z$  80 and  $m/z$  66.

directly from **IV** and **V** as the TS energies for the requisite 1-4 C-O H shift are too high. Similarly, the TS energies for the direct unimolecular isomerisation of the two structures are too high at  $190 \text{ kJ mol}^{-1}$  for both ions.

#### 4. Discussion

The most important and surprising experimental observation in this work is that both  $\alpha$  and  $\beta$  H/D elimination from the ethyl moiety occur when eliminating ethene from the parent ions **IV** and **V** (see Fig. 1). Although the observed branching ratios are not indicative of the true branching ratios because of the rapid D/H exchange with water in the buffer gas occurring in the product ions, simulation of the kinetics suggests that  $\alpha$ -elimination

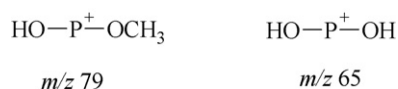


Fig. 17. Isomeric structures of the isotopomeric ions in Fig. 16.

is more difficult than  $\beta$ -elimination. These simulations ignore kinetic isotope effects but the results of the DFT calculations indicate that they are likely to be marginal compared to the differences in the TS energies of the two pathways. As both pathways lead to the same products (ignoring isotopic labelling) and thus have the same overall energetics, that we observe a non-unitary branching ratio supports the proposal that entropic contributions to the fragmentation processes cannot be ignored although their contributions to the steps prior to the dissociation of the complex are relatively minor.

DFT calculations were used to investigate the likely mechanisms of the eliminations of ethene. They showed that, as was found in the study of dimethyl methylphosphonate, only alkyl migration from phosphorus to oxygen, and hydrogen migration to phosphorus occur. This was particularly surprising in view of the possibility of the 1,4 C-O H shift involving a 5-membered transition state for the direct elimination of ethene from either **IV** or **V**.

#### Acknowledgements

Support from the EC “Reactive Intermediates” Research Training Network and the Leverhulme Trust and from the Ministero dell’Istruzione, dell’Università e della Ricerca, MIUR is gratefully acknowledged. We thank Centro Universitario di Calcolo for the computer time on the Linux cluster.

#### References

- [1] A.J. Bell, D. Despeyroux, J. Murrell, P. Watts, *Int. J. Mass. Spectrom. Ion. Proc.* 165/166 (1997) 5333.
- [2] J.D. Barr, A.J. Bell, D.O. Konn, J. Murrell, C.M. Timperley, M.J. Waters, P. Watts, *Phys. Chem. Chem. Phys.* 4 (2002) 2200.
- [3] A.J. Bell, A. Citra, J.M. Dyke, F. Ferrante, L. Gagliardi, P. Watts, *Phys. Chem. Chem. Phys.* 6 (2004) 2200.
- [4] A. Michaelis, T. Becker, *Chem. Ber.* 30 (1897) 1003.
- [5] L.G. Spears, A. Liao, D. Minsek, E.S. Lewis, *J. Org. Chem.* 52 (1987) 61.
- [6] A.D. Becke, *J. Chem. Phys.* 98 (1993) 5648.
- [7] M.J. Frisch, G.W. Trucks, H.B. Schlegel, G.E. Scuseria, M.A. Robb, J.R. Cheeseman, J.A. Montgomery Jr., T. Vreven, K.N. Kudin, J.C. Burant, J.M. Millam, S.S. Iyengar, J. Tomasi, V. Barone, B. Mennucci, M. Cossi, G. Scalmani, N. Rega, G.A. Petersson, H. Nakatsuji, M. Hada, M. Ehara, K. Toyota, R. Fukuda, J. Hasegawa, M. Ishida, T. Nakajima, Y. Honda, O. Kitao, H. Nakai, M. Klene, X. Li, J.E. Knox, H.P. Hratchian, J.B. Cross, C. Adamo, J. Jaramillo, R. Gomperts, R.E. Stratmann, O. Yazyev, A.J. Austin, R. Cammi,



C. Pomelli, J.W. Ochterski, P.Y. Ayala, K. Morokuma, G.A. Voth, P. Salvador, J.J. Dannenberg, V.G. Zakrzewski, S. Dapprich, A.D. Daniels, M.C. Strain, O. Farkas, D.K. Malick, A.D. Rabuck, K. Raghavachari, J.B. Foresman, J.V. Ortiz, Q. Cui, A.G. Baboul, S. Clifford, J. Cioslowski, B.B. Stefanov, G. Liu, A. Liashenko, P. Piskorz, I. Komaromi, R.L. Martin, D.J. Fox, T. Keith,

M.A. Al-Laham, C.Y. Peng, A. Nanayakkara, M. Challacombe, P.M.W. Gill, B. Johnson, W. Chen, M.W. Wong, C. Gonzalez, J.A. Pople, Gaussian 03, *Revision C. 01*, Gaussian Inc., Wallingford CT, 2004.  
[8] J.D. Barr, A.J. Bell, F. Ferrante, G. La Manna, J.L. Mundy, C.M. Timperley, M.J. Waters, P. Watts, *Int. J. Mass. Spectrom. Ion. Proc.* 244 (2005)29.